Exact solution of the Bloch equations for the nonresonant exponential model in the presence of dephasing

K. N. Zlatanov,[1,2] G. S. Vasilev,[1] P. A. Ivanov,[1] and N. V. Vitanov[1]
[1]*Department of Physics, Sofia University, James Bourchier 5 blvd, 1164 Sofia, Bulgaria*
[2]*Institute of Solid State Physics, Bulgarian Academy of Sciences, Tsarigradsko chaussée 72, 1784 Sofia, Bulgaria*
(Received 11 August 2015; published 6 October 2015)

An exact analytic solution is presented for a two-state quantum system driven by a time-dependent external field with an exponential temporal shape in the presence of dephasing. In the absence of dephasing the model reduces to the well-known Demkov model originally introduced in slow atomic collisions. The solution is expressed in terms of the generalized hypergeometric function ${}_1F_2(a;b_1,b_2;x)$. Various limiting cases are examined in the limits of weak and strong dephasing, strong driving field, and exact resonance.

DOI: 10.1103/PhysRevA.92.043404 PACS number(s): 32.80.Qk, 32.80.Xx, 34.70.+e, 03.65.Aa

I. INTRODUCTION

The two-state quantum system is a fundamental object in time-dependent quantum mechanics. It is not only the qubit in quantum information, but it is also the foundation for understanding of a variety of phenomena in areas ranging from nuclear magnetic resonance, quantum optics, atomic collisions, and condensed matter to polarization optics, waveguide optics, frequency conversion, and even neutrino oscillations. Moreover, multistate quantum dynamics can often be understood only if reduced to one or more two-state problems via an appropriate transformation [1,2]. Besides the simple case of exact resonance between the frequency of the external driving field and the system frequency, the two-state time-dependent Schrödinger equation (TDSE) has exact analytic solutions for several off-resonant models [1]. These include the Rabi [3], Landau-Zener-Stückelberg-Majorana [4–7], Rosen-Zener [8], Demkov [9,10], Nikitin [11,12], Allen-Eberly [13,14], Bambini-Berman [15], Demkov-Kunike [16–19], and Carrol-Hioe [20] models, the recently solved tanh model [21], etc. Because TDSE can be cast into a second-order ordinary differential equation vs time, all of these models but the Rabi model express the respective solution in terms of a special function, which solves a second-order ordinary differential equation: the Weber parabolic cylinder function (Landau-Zener-Stückelberg-Majorana model), the Bessel function (Demkov model), the Gauss hypergeometric function (Rosen-Zener, Allen-Eberly, Bambini-Bermann, Demkov-Kunike, Carroll-Hioe models), the Kummer confluent hypergeometric function (Nikitin model), associated Legendre functions (tanh model), etc. A different approach has been used by Barnes and Das Sarma [22], and recently by Vitanov and Shore [23], who derived a variety of soluble models by assuming that the solution is known and considered TDSE as an equation for the field.

All these analytic solutions assume coherent excitation, i.e., any decoherence is completely absent. In other words, they apply to cases when the interaction duration is much shorter than the decoherence times of the system. In the presence of decoherence effects, such as spontaneous emission and collisional dephasing, TDSE is replaced by the three coupled Bloch equations [1,13,24,25]. Hence the inclusion of decoherence requires the solution of a differential equation of *third* order, which is far more demanding. Therefore, exact analytic solutions in the presence of decoherence are nearly absent. A notable exception is the Rabi model, which assumes a driving field of rectangular shape and a constant detuning; hence it is described by a differential equation with constant coefficients that is readily solved even with decoherence [1]. Another exact solution is the on-resonance Rosen-Zener model with dephasing [26], in which, due to the resonance (zero detuning), one of the Bloch equations decouples and we are left with only two coupled Bloch equations that result in a single second-order differential equation.

We note that the Bloch equations can be solved approximately in the limits of weak and strong dephasing rates [27–29]. These approximate analytic solutions apply to rather general temporal dependences of the Hamiltonian elements and provide reasonable approximations to the exact solutions.

In this paper, we consider the simplest form of decoherence—pure dephasing (also known as transverse relaxation)—which is described by the T_2^* time in the Bloch equations. We derive an exact analytical solution for a model with a nonzero detuning and a coupling of exponential time dependence in the presence of dephasing. This is possible because the Bloch equations for this model can be cast into a third-order ordinary differential equation that is satisfied by a generalized hypergeometric function [30,31]. In the absence of dephasing this model reduces to the Demkov model for noncrossing energy levels, which has been introduced in the theory of slow atomic collisions [9,10]. This exponential model still remains a popular model for effective two-level problems in quantum metrology [32,33] and quantum simulations [34–36] because the exponentially decreasing pulse shape allows one to gradually decrease the field and pass through a quantum phase transition. Here we report the effects of dephasing on the transition probabilities, which are highly relevant to quantum protocols insofar as the latter often have to account for a noisy environment.

This paper is organized as follows. In Sec. II we define the dissipative exponential model. In Sec. III we derive the exact solution of this model in terms of generalized hypergeometric functions and explore various limiting cases of weak and strong dephasing and strong field. In Sec. IV we derive and examine the solution in the case of exact resonance. Finally, in Sec. V we present a summary.

II. DISSIPATIVE EXPONENTIAL MODEL

To be specific, among the variety of two-state systems in quantum physics we consider a two-state atom with internal states $|1\rangle$ and $|2\rangle$ and transition frequency ω_0, which interacts with a laser field with a carrier frequency ω_l. We shall use the language of laser-atom excitation although the results are valid for any two-level system driven by an external field. There are many situations when pure dephasing, without population redistribution (e.g., by spontaneous emission), takes place. An immediate example is the collective dephasing experienced by an inhomogeneously broadened atomic ensemble. Such dephasing takes place in doped solids on the microsecond scale, while the population lifetimes of metastable levels used for optical data storage are on the minute scale [37]. Another example is collisional dephasing in atomic vapors, which is not accompanied by population changes. Yet another example is the phase fluctuations of the driving field (laser or microwave), which cause dephasing of the atomic coherence but no population changes.

In the rotating-wave approximation, the Hamiltonian describing the laser-atom interaction is given by [1,13]

$$\mathbf{H}(t) = \frac{\hbar\Delta(t)}{2}\boldsymbol{\sigma}_z + \frac{\hbar\Omega(t)}{2}\boldsymbol{\sigma}_x, \tag{1}$$

where $\boldsymbol{\sigma}_k$ $(k = x,y,z)$ are the Pauli matrices, and $\Delta(t) = \omega_0 - \omega_l$ is the system-field detuning. $\Omega(t)$ is the time-dependent Rabi frequency, which is proportional to the laser-atom interaction, $\Omega(t) = -\mathbf{d}\cdot\mathbf{E}(t)/\hbar$, with $\mathbf{d}$ being the transition electric dipole moment and $\mathbf{E}(t)$ the electric field envelope.

We model the time evolution of the density operator $\boldsymbol{\rho}$ for the two-state system in the presence of dephasing by the following master equation:

$$\frac{d}{dt}\boldsymbol{\rho}(t) = -i[\mathbf{H},\boldsymbol{\rho}] + \frac{\Gamma}{2}(\boldsymbol{\sigma}_z\boldsymbol{\rho}\boldsymbol{\sigma}_z - \boldsymbol{\rho}), \tag{2}$$

where Γ is the constant dephasing rate ($\Gamma \geqq 0$) and $T_2^* = 1/\Gamma$ is the decoherence time. It is convenient to treat the dissipative dynamics in terms of the Bloch vector $\mathbf{B}(t) = [u(t),v(t),w(t)]^T$, where

$$u(t) = 2\,\mathrm{Re}\boldsymbol{\rho}_{12}(t), \tag{3a}$$

$$v(t) = 2\,\mathrm{Im}\boldsymbol{\rho}_{12}(t), \tag{3b}$$

$$w(t) = \boldsymbol{\rho}_{22}(t) - \boldsymbol{\rho}_{11}(t), \tag{3c}$$

with $\boldsymbol{\rho}_{ij}(t) = \langle i|\boldsymbol{\rho}(t)|j\rangle$. The Bloch vector components obey the Bloch equations [1,13],

$$\frac{d}{dt}\begin{bmatrix} u(t)\\ v(t)\\ w(t)\end{bmatrix} = \begin{bmatrix} -\Gamma & -\Delta & 0\\ \Delta & -\Gamma & -\Omega(t)\\ 0 & \Omega(t) & 0\end{bmatrix}\begin{bmatrix} u(t)\\ v(t)\\ w(t)\end{bmatrix}. \tag{4}$$

Due to its significance in practical applications we consider only the interval $t \in [0,+\infty)$. The Rabi frequency in this interval and the detuning for the Demkov model are given by

$$\Omega(t) = \Omega_0 e^{-t/T}, \quad \Delta = \text{const}. \tag{5}$$

Here Ω_0 is the peak Rabi frequency, which we assume positive without loss of generality and T is the characteristic pulse width. For $\Gamma = 0$, the Bloch equation (4) is solved exactly and the solution represents the well known Demkov model [9] introduced in the theory of slow atomic collisions over 50 years ago.

Our objective is to find the population inversion $w(+\infty)$ at $t \to \infty$ for the most common initial conditions at $t = 0$: the system initially in the ground state $|1\rangle$, or in an equal coherent superposition of states $|1\rangle$ and $|2\rangle$.

III. EXACT SOLUTION

A. General solution

We begin by decoupling the equation for the population inversion $w(t)$ from the Bloch equations (4) by repeated differentiation and substitution. The result is the linear third-order ordinary differential equation

$$\dddot{w} + 2(T^{-1}+\Gamma)\ddot{w} + \left[(T^{-1}+\Gamma)^2 + \Delta^2 + \Omega_0^2 e^{-2t/T}\right]\dot{w} + \Omega_0^2(\Gamma - T^{-1})e^{-2t/T}w = 0, \tag{6}$$

where an overdot denotes a time derivative. We introduce the dimensionless parameters

$$\gamma = \frac{\Gamma T}{2}, \quad \delta = \frac{\Delta T}{2}, \quad \alpha = \frac{\Omega_0 T}{2}, \tag{7}$$

and we change the independent variable from t to

$$x(t) = -\Omega(t)^2 T^2/4 = -\alpha^2 e^{-2t/T}. \tag{8}$$

Note that $x(0) = -\alpha^2 = x_0$ and $x(+\infty) = 0$. In terms of x, Eq. (6) is transformed into the generalized hypergeometric equation [30,31],

$$x^2 W'''(x) + (b_1 + b_2 + 1)xW''(x) + (b_1 b_2 - x)W'(x) - aW(x) = 0, \tag{9}$$

with $' \equiv d/dx$, $W(x) = w(t(x))$, and

$$a = \tfrac{1}{2} - \gamma, \quad b_1 = \tfrac{1}{2} - \gamma + i\delta, \quad b_2 = \tfrac{1}{2} - \gamma - i\delta. \tag{10}$$

The solution of Eq. (9) is expressed in terms of the generalized hypergeometric function (GHF) ${}_1F_2(a;b_1,b_2;x)$ [not to be confused with the Gauss hypergeometric function ${}_2F_1(a_1,a_2;b;x)$, which satisfies a second-order differential equation]. This equation possesses three independent solutions,

$$f_1(x) = {}_1F_2\left(\tfrac{1}{2}-\gamma;\tfrac{1}{2}-\gamma-i\delta,\tfrac{1}{2}-\gamma+i\delta;x\right), \tag{11a}$$

$$f_2(x) = x^{\frac{1}{2}+\gamma+i\delta}\,{}_1F_2\left(1+i\delta;1+2i\delta,\tfrac{3}{2}+\gamma+i\delta;x\right), \tag{11b}$$

$$f_3(x) = x^{\frac{1}{2}+\gamma-i\delta}\,{}_1F_2\left(1-i\delta;1-2i\delta,\tfrac{3}{2}+\gamma-i\delta;x\right). \tag{11c}$$

Hence the general solution for the population inversion is

$$W(x) = Af_1(x) + Bf_2(x) + Cf_3(x), \tag{12}$$

where A, B, and C are integration constants. We determine them from the initial conditions,

$$A = \frac{1}{\mathcal{W}}\begin{vmatrix} W & f_2 & f_3\\ W' & f_2' & f_3'\\ W'' & f_2'' & f_3''\end{vmatrix}, \quad B = \frac{1}{\mathcal{W}}\begin{vmatrix} f_1 & W & f_3\\ f_1' & W' & f_3'\\ f_1'' & W'' & f_3''\end{vmatrix},$$

$$C = \frac{1}{\mathcal{W}}\begin{vmatrix} f_1 & f_2 & W\\ f_1' & f_2' & W'\\ f_1'' & f_2'' & W''\end{vmatrix}, \tag{13}$$

where all functions are evaluated at $x = x_0 = -\alpha^2$. The denominator $\mathcal{W}$ of the expressions for A, B, and C is the Wronskian of the three solutions f_1, f_2, and f_3, which is (see the Appendix)

$$\mathcal{W}\{f_1(x), f_2(x), f_3(x)\} = -2i\delta x^{2(\gamma-1)}\big[(\gamma+\tfrac{1}{2})^2+\delta^2\big]. \quad (14)$$

Of special interest is the value of the population inversion at $t \to \infty$. Because $x(\infty) = 0$, and in view of Eq. (A5) and $\gamma \geqq 0$, we find that two of the independent solutions vanish in this limit: $f_2(0) = f_3(0) = 0$, while $f_1(0) = 1$. Therefore, at the end of the interaction ($t \to \infty$) we have

$$w(\infty) = W(0) = A. \quad (15)$$

This equation is valid for any initial condition. However, the initial conditions still influence the final population inversion through the values of $W(x)$ and its derivatives at x_0 that are contained in the coefficient A; see Eq. (13). The values of the derivatives are readily found from the initial values of the Bloch vector components $U(x_0)$, $V(x_0)$, and $W(x_0)$, taking into account the relation $\dot{x} = -2x/T$,

$$W'(x_0) = \frac{V(x_0)}{\alpha}, \quad (16a)$$

$$W''(x_0) = \frac{\delta U(x_0) + \big(\frac{1}{2}-\gamma\big)V(x_0) - \alpha W(x_0)}{\alpha^3}. \quad (16b)$$

B. System initially in state |1⟩

When the system starts in state $|1\rangle$ at time $t = 0$, the Bloch variables have the initial values $U(x_0) = V(x_0) = 0$, $W(x_0) = -1$. Then, looking back at Eqs. (16), we find $W'(x_0) = 0$ and $W''(x_0) = 1/\alpha^2$. We are interested in the population inversion $w(\infty) = W(0)$ at $t \to \infty$ (meaning $x = 0$); hence all asymptotics below are derived at this limit. Equations (13), (14), and (15) give

$$W(0) = \frac{i x_0^{2(1-\gamma)}}{2\delta\big[\big(\gamma+\frac{1}{2}\big)^2+\delta^2\big]}\begin{vmatrix} -1 & f_2 & f_3 \\ 0 & f_2' & f_3' \\ 1/\alpha^2 & f_2'' & f_3'' \end{vmatrix}_{x_0}, \quad (17)$$

where the functions $f_2(x)$ and $f_3(x)$ and their derivatives are taken at the initial point $x_0 = -\alpha^2$.

Now we turn our attention to several limiting cases of the exact formula (17), which allow us to derive simpler approximate expressions.

1. Asymptotics for $\gamma \ll 1$

The straightforward way of deriving the asymptotic solution in the weak-dephasing limit is by expanding Eq. (15) in Taylor series around $\gamma = 0$,

$$w(\infty) \sim w_0(\infty) + \gamma\left(\frac{dA}{d\gamma}\right)_{\gamma=0} + O(\gamma^2). \quad (18)$$

The first term on the right-hand side, $w_0(\infty) = (A)_{\gamma=0}$, gives the exact solution obtained for zero dephasing [38],

$$w_0(\infty) \sim \frac{\pi\alpha}{2\cosh(\pi\delta)}\big[|J_{\frac{1}{2}-i\delta}(\alpha)|^2 - |J_{-\frac{1}{2}+i\delta}(\alpha)|^2\big]. \quad (19)$$

The second term in Eq. (18) does not have a simple compact form due to the cumbersome derivatives of the GHF with respect to its parameters (see the Appendix); it can be computed by using Eq. (A1).

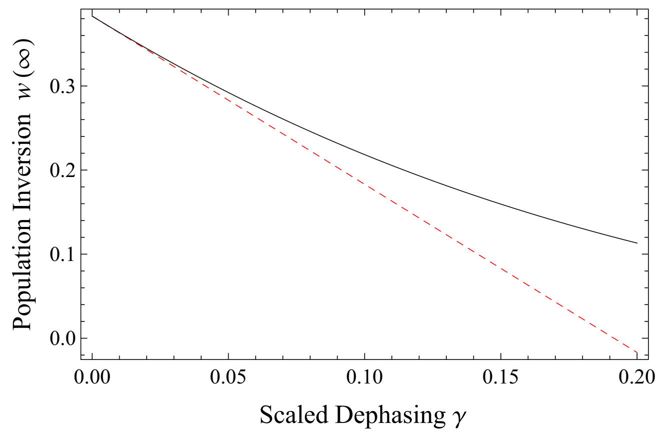

FIG. 1. (Color online) Population inversion vs the scaled dephasing rate $\gamma = \Gamma T/2$ in the weak-dephasing regime, $\gamma \ll 1$. The interaction parameters are $\delta = 0.35$ and $\alpha = 20$. The asymptotic solution (18) is plotted by the dashed curve and the exact solution (17) is plotted by the solid curve.

Figure 1 compares the asymptotic formula (18) to the exact solution (17) at $t \to \infty$. As expected, the asymptotic formula is very accurate for small values of γ.

2. Asymptotics for $\gamma \gg 1$

In the limit $\gamma \gg 1$, we first simplify the exact formula (17). This formula involves the functions $f_2(x)$ and $f_3(x)$ as well as their first and second derivatives, all estimated at the initial point $x_0 = -\alpha^2$. In the limit $\gamma \gg 1$ we retain only the leading terms in γ in the derivatives,

$$f_2'(x_0) \sim \big(\tfrac{1}{2}+\gamma+i\delta\big)x_0^{-\frac{1}{2}+\gamma+i\delta} \times {}_1F_2\big(1+i\delta; 1+2i\delta, \tfrac{3}{2}+\gamma+i\delta; x_0\big), \quad (20a)$$

$$f_3'(x_0) \sim \big(\tfrac{1}{2}+\gamma-i\delta\big)x_0^{-\frac{1}{2}+\gamma-i\delta} \times {}_1F_2\big(1-i\delta; 1-2i\delta, \tfrac{3}{2}+\gamma-i\delta; x_0\big), \quad (20b)$$

$$f_2''(x_0) \sim \big(\tfrac{1}{2}+\gamma+i\delta\big)\big(-\tfrac{1}{2}+\gamma+i\delta\big)x_0^{-\frac{3}{2}+\gamma+i\delta} \times {}_1F_2\big(1+i\delta; 1+2i\delta, \tfrac{3}{2}+\gamma+i\delta; x_0\big), \quad (20c)$$

$$f_3''(x_0) \sim \big(\tfrac{1}{2}+\gamma-i\delta\big)\big(-\tfrac{1}{2}+\gamma-i\delta\big)x_0^{-\frac{3}{2}+\gamma-i\delta} \times {}_1F_2\big(1-i\delta; 1-2i\delta, \tfrac{3}{2}+\gamma-i\delta; x_0\big). \quad (20d)$$

Furthermore, we neglect the term $1/\alpha^2$ in the determinant in Eq. (17) because it is associated with products of HGFs, which have large-γ asymptotics of higher order compared to the ones associated with the term -1. We thereby obtain

$$w(\infty) \sim i\,\frac{f_2''(x_0)f_3'(x_0) - f_3''(x_0)f_2'(x_0)}{2\delta x_0^{2(\gamma-1)}\big[\big(\gamma+\frac{1}{2}\big)^2+\delta^2\big]}, \quad (21)$$

and after a simple algebra we find

$$w(\infty) \sim -\big|{}_1F_2\big(1+i\delta; 1+2i\delta, \tfrac{3}{2}+\gamma+i\delta; x_0\big)\big|^2. \quad (22)$$

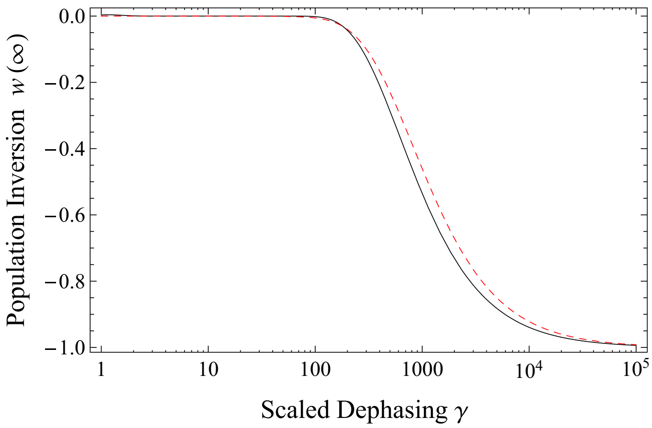

FIG. 2. (Color online) Population inversion vs scaled dephasing rate $\gamma = \Gamma T/2$ in the strong-dephasing regime ($\gamma \gg 1$). The interaction parameters are $\delta = 0.75$ and $\alpha = 25$. The asymptotic solution (22) is plotted by the dashed curve and the exact solution (17) is plotted by the solid curve.

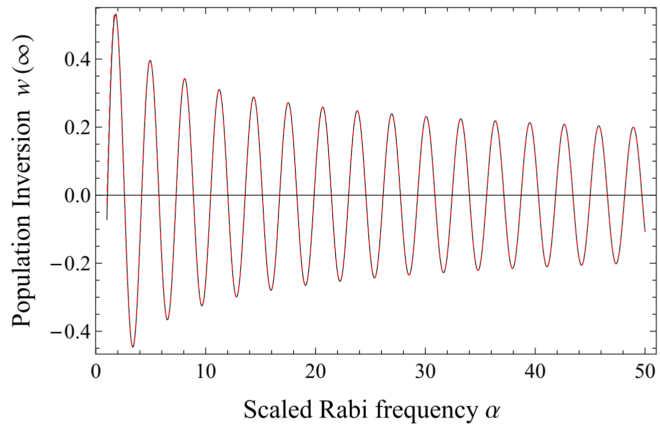

FIG. 3. (Color online) Population inversion vs scaled Rabi frequency $\alpha = \Omega_0 T/2$ in the strong-coupling regime ($\alpha \gg 1$). The interaction parameters are $\delta = 0.1$ and $\gamma = 0.3$. The asymptotic solution (25) is plotted by the dashed curve and the exact solution (17) is plotted by the solid curve; the two curves are nearly indiscernible.

It follows immediately that for large γ the inversion cannot be positive: $w \leqq 0$.

A further approximation can be derived from here by using the power series expansion versus x_0 of the HGF involved; it reads

$$w(\infty) \sim -1 + \frac{\alpha^2}{\gamma} - \frac{\alpha^4}{2\gamma^2} + \frac{\alpha^6}{6\gamma^3} - \frac{\alpha^8}{24\gamma^4} + \cdots . \quad (23)$$

This expansion is useful for $\alpha^2 \ll \gamma$. Not surprisingly, this is exactly the expansion of the function

$$w(\infty) \sim -e^{-\alpha^2/\gamma}. \quad (24)$$

This has to be expected from the general formulas for an arbitrary Hamiltonian [28,29].

Figure 2 shows a comparison between the asymptotic and numerical solutions of Eq. (6). The analytic approximation (22) matches the exact result (17) very closely. As evident, increasing of the dephasing after a certain value decouples the system and returns it to the ground state, which is a manifestation of quantum overdamping [39].

3. *Asymptotics for α ≫ 1*

In the limit $\alpha \gg 1$, we replace the GHFs in Eq. (17) with their large-argument asymptotics (A8), and find

$$w(\infty) \sim -\alpha^{-\gamma} \cos\left(2\alpha - \tfrac{1}{2}\pi\gamma\right) \frac{\left|\Gamma\left(\frac{1}{2} + \gamma + i\delta\right)\right|^2}{\sqrt{\pi}\,\Gamma\left(\frac{1}{2} + \gamma\right)}. \quad (25)$$

In the limit $\gamma \to 0$ we obtain

$$w(\infty) \sim -\frac{\cos(2\alpha)}{\cosh(\pi\delta)}. \quad (26)$$

Figure 3 shows a comparison of the asymptotic expansion (25) and the exact formula (17) in this regime. A nearly perfect agrement is observed, with the asymptotic and exact results barely discernible.

C. System initially in a maximally coherent superposition of states

Another interesting case, which is of potential significance in quantum metrology [32], is when the system is prepared initially in a coherent superposition of the two states. When the system starts its evolution in the equal coherent superposition $(|1\rangle + |2\rangle)/\sqrt{2}$ at time $t = 0$, the Bloch variables have the initial values $U(x_0) = 1$, $V(x_0) = W(x_0) = 0$. Then Eq. (16) gives $W'(x_0) = 0$ and $W''(x_0) = \delta/\alpha^3$. Therefore, Eqs. (13), (14), and (15) give

$$w(\infty) = i\,\frac{f_2(x_0) f_3'(x_0) - f_2'(x_0) f_3(x_0)}{2\alpha^3 x_0^{2(\gamma-1)}\left[\left(\gamma + \frac{1}{2}\right)^2 + \delta^2\right]}. \quad (27)$$

The asymptotic behavior of this expression for large values of $|x_0| = \alpha^2$ is found from the respective asymptotic expansions of the GHF $f_2(x_0)$ and $f_3(x_0)$ involved; it reads

$$w(\infty) \sim -\frac{\sinh(\pi\delta)}{\pi\alpha^{2\gamma}}\left|\Gamma\left(\tfrac{1}{2} + \gamma + i\delta\right)\right|^2 \quad (\alpha \gg 1). \quad (28)$$

For small and large values of the dephasing rate γ this expression is further simplified to

$$w(\infty) \sim -\frac{\tanh(\pi\delta)}{\alpha^{2\gamma}}\left[1 + 2\gamma\,\mathrm{Re}\,\psi\left(\tfrac{1}{2} + i\delta\right)\right] \quad (\gamma \ll 1), \quad (29a)$$

$$w(\infty) \sim -2e^{-2\gamma}\left(\frac{\gamma}{\alpha}\right)^{2\gamma} \sinh(\pi\delta) \quad (\gamma \gg 1). \quad (29b)$$

Here $\psi(z)$ is Euler's ψ (digamma) function.

Figure 4 shows a comparison between the asymptotic formula (28) and the exact formula (27). With the exception of the small-amplitude oscillations, the asymptotic formula (28) is very accurate across the range.

IV. EXACT RESONANCE

It is now instructive to investigate the resonant regime of the dissipative Demkov model, as has been done earlier for the

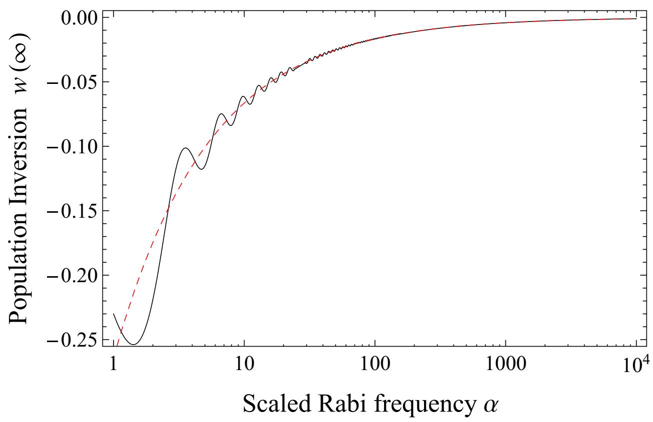

FIG. 4. (Color online) Population inversion vs scaled Rabi frequency $\alpha = \Omega_0 T/2$ in the range $\alpha \gg 1$ in the case when the system is initially in a coherent superposition of states, $w(0) = 0$. The other parameters are $\gamma = 0.3$ and $\delta = 0.2$. The asymptotic solution (28) is plotted by the dashed curve and the exact solution (27) is plotted by the solid curve.

dissipative Rosen-Zener model [26]. In this simplified case the Bloch equations take the form

$$\frac{d}{dt}u(t) = -\Gamma u(t), \tag{30a}$$

$$\frac{d}{dt}\begin{bmatrix} v(t) \\ w(t) \end{bmatrix} = \begin{bmatrix} -\Gamma & -\Omega(t) \\ \Omega(t) & 0 \end{bmatrix}\begin{bmatrix} v(t) \\ w(t) \end{bmatrix}. \tag{30b}$$

Now the Bloch equations factorize into a single equation for the coherence $u(t)$, and a system of two equations for the remaining components of the Bloch vector $v(t)$ and $w(t)$. The solution can be derived by reducing Eq. (30b) to a single second-order differential equation for $w(t)$. However, it can also be obtained from the general solution in the off-resonance case derived above.

By setting $\delta = 0$ in Eqs. (11) we find

$$\begin{aligned} g_1(x) &= f_1(x)\big|_{\delta=0} = {}_1F_2\left(\tfrac{1}{2}-\gamma; \tfrac{1}{2}-\gamma, \tfrac{1}{2}-\gamma; x\right) \\ &= {}_0F_1\left(; \tfrac{1}{2}-\gamma; x\right) \\ &= (-x)^{(\frac{1}{2}+\gamma)/2}\Gamma\left(\tfrac{1}{2}-\gamma\right)J_{-\frac{1}{2}-\gamma}(2\sqrt{-x}), \end{aligned} \tag{31a}$$

$$\begin{aligned} g_2(x) &= f_2(x)\big|_{\delta=0} = x^{\frac{1}{2}+\gamma}\, {}_1F_2\left(1; 1, \tfrac{3}{2}+\gamma; x\right) \\ &= x^{\frac{1}{2}+\gamma}\, {}_0F_1\left(; \tfrac{3}{2}+\gamma; x\right) \\ &= (-x)^{(\frac{1}{2}+\gamma)/2}\Gamma\left(\tfrac{3}{2}+\gamma\right)J_{\frac{1}{2}+\gamma}(2\sqrt{-x}). \end{aligned} \tag{31b}$$

Here we have used the relations [30]

$${}_1F_2(a; a, b; x) = {}_0F_1(b; x) = \Gamma(b)(-x)^{\frac{1-b}{2}}J_{b-1}(2\sqrt{-x}), \tag{32}$$

with $J_\nu(z)$ being the Bessel function of the first kind. At the initial moment $x_0 = -\alpha^2$ we find

$$g_1(x_0) = \alpha^{\frac{1}{2}+\gamma}\Gamma\left(\tfrac{1}{2}-\gamma\right)J_{-\frac{1}{2}-\gamma}(2\alpha), \tag{33a}$$

$$g_2(x_0) = \alpha^{-\frac{1}{2}-\gamma}\Gamma\left(\tfrac{3}{2}+\gamma\right)J_{\frac{1}{2}+\gamma}(2\alpha), \tag{33b}$$

while at the final moment $x = 0$ we have

$$g_1(0) = 1, \quad g_2(0) = 0, \tag{34}$$

where we have used the property ${}_0F_1(; b; 0) = 1$. Therefore, the solution on resonance reads

$$W(x) = Dg_1(x) + Eg_2(x), \tag{35}$$

with

$$D = \frac{\begin{vmatrix} W(x_0) & g_2(x_0) \\ W'(x_0) & g_2'(x_0) \end{vmatrix}}{\mathcal{W}[g_1(x_0), g_2(x_0)]}, \tag{36a}$$

$$E = \frac{\begin{vmatrix} g_1(x_0) & W(x_0) \\ g_1'(x_0) & W'(x_0) \end{vmatrix}}{\mathcal{W}[g_1(x_0), g_2(x_0)]}. \tag{36b}$$

The Wronskian has the exact value

$$\mathcal{W}[g_1(x), g_2(x)] = \left(\gamma + \tfrac{1}{2}\right)x^{\gamma-\frac{1}{2}}. \tag{37}$$

In the end on the interaction, at $x = 0$, the final population inversion reads

$$W(0) = Dg_1(0) + Eg_2(0) = D = \frac{x_0^{\frac{1}{2}-\gamma}}{\gamma + \frac{1}{2}}\begin{vmatrix} W(x_0) & g_2(x_0) \\ W'(x_0) & g_2'(x_0) \end{vmatrix}. \tag{38}$$

When the system starts its evolution in the ground state $|1\rangle$, we have, according to Eq. (16), $W(x_0) = -1$ and $W'(x_0) = 0$.

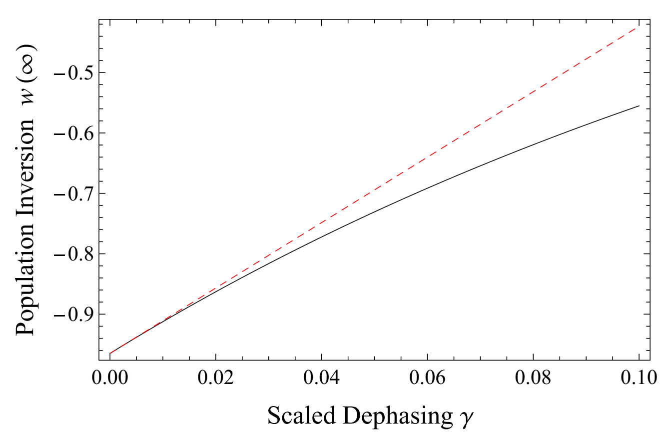

FIG. 5. (Color online) Population inversion vs scaled dephasing $\gamma = \Gamma T/2$ in the weak-dephasing regime ($\gamma \ll 1$) on exact resonance ($\delta = 0$). The asymptotic solution (40) is plotted by the dashed curve and the exact solution (39) is plotted by the solid curve. The scaled Rabi frequency is $\alpha = 25$.

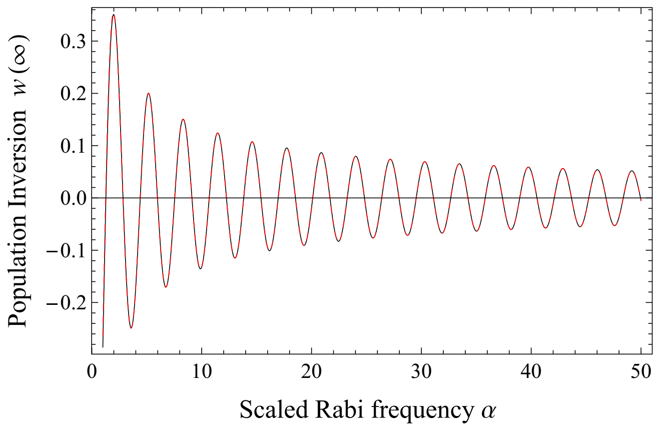

FIG. 6. (Color online) Population inversion vs scaled Rabi frequency $\alpha = \Omega_0 T/2$ in the large-coupling regime ($\alpha \gg 1$) on exact resonance ($\delta = 0$). The asymptotic solution (42) is plotted by the dashed curve and the exact solution (39) is plotted by the solid curve. The two curves are almost indiscernible. The scaled dephasing rate is $\gamma = 0.6$.

Hence

$$w(\infty) = -\frac{g_2'(x_0)x_0^{\frac{1}{2}-\gamma}}{\gamma+\frac{1}{2}} = -{}_0F_1\left(;\tfrac{1}{2}+\gamma;-\alpha^2\right) = -\Gamma\left(\gamma+\tfrac{1}{2}\right)\alpha^{\frac{1}{2}-\gamma} J_{\gamma-\frac{1}{2}}(2\alpha). \quad (39)$$

1. Asymptotic behavior for $\gamma \ll 1$

The asymptotics for $\gamma \ll 1$ is derived by using Eq. (39), and expanding the Bessel function and the pre-factors in Taylor series versus γ. The result is

$$w(\infty) \sim -\cos(2\alpha) + \{\cos(2\alpha)[C - \mathrm{Ci}(4\alpha) + \log(4\alpha)] - \sin(2\alpha)\mathrm{Si}(4\alpha\}\gamma. \quad (40)$$

Here $\mathrm{Ci}(4\alpha)$ and $\mathrm{Si}(4\alpha)$ are the cosine and sine integrals, while $C = 0.5772\ldots$ is the Euler's constant. Figure 5 compares this approximation with the exact values in this weak-dephasing regime.

2. Asymptotic behavior for $\gamma \gg 1$

For large γ we expand the HGF in Eq. (39) in power series versus α, which is rapidly converging for $\gamma \gg 1$ because in this limit the series turns into a series in α^2/γ. The result is the same as in the nonresonant case, Eqs. (23) and (24).

3. Asymptotic behavior for $\alpha \gg 1$

In the limit of large α, we use the well-known asymptotics of the Bessel function [30] in Eq. (39),

$$J_\nu(z) \sim \sqrt{\frac{2}{\pi z}}\cos[z-(2\nu+1)\pi/4] \quad (|\arg(z)| < \pi,\ |z| \to \infty). \quad (41)$$

The asymptotics of the population inversion reads

$$w(\infty) \sim -\Gamma\left(\gamma+\tfrac{1}{2}\right)\frac{\alpha^{-\gamma}}{\sqrt{\pi}}\cos(2\alpha - \gamma\pi/2). \quad (42)$$

This approximate formula is compared to the exact values in Fig. 6. A perfect agreement is observed throughout the entire range $\alpha \gtrsim 1$: the two curves are indiscernible.

V. CONCLUSIONS

In this paper, we have derived and studied the exact analytic solution of the Bloch equations for a two-state quantum system driven by an external field of exponential time dependence in the presence of dephasing process. In the absence of dephasing this model is the well-known Demkov model originally introduced in the theory of slow atomic collisions. Contrary to previous solutions for other models that considered only the case of exact resonance between the carrier frequency of the driving field and the Bohr transition frequency of the system, here we derived the solution in the general case of arbitrary nonzero detuning. The implication is that we had to deal with all three Bloch equations that result in a third-order differential equation for the population inversion. The solution is expressed in terms of the generalized hypergeometric function ${}_1F_2(a;b_1,b_2;x)$. By using the series expansions and the asymptotics of this function versus its parameters we have derived the behavior of the population inversion in various limiting cases of physical interest, such as weak and strong dephasing, strong driving field, and exact resonance. The results are of potential interest to a variety of physical problems involving qubits driven by an external field in a noisy environment, e.g., in quantum metrology [32,33] and quantum simulations [34–36].

ACKNOWLEDGMENT

This work has been supported by the European Reintegration Grant (ERG) No. PERG07-GA-2010-268432 (QUANTNET).

APPENDIX: RELEVANT PROPERTIES OF ${}_1F_2(a;b_1,b_2;x)$

For the sake of readers convenience we summarize here some relevant properties of the generalized hypergeometric function ${}_1F_2(a;b_1,b_2;x)$. Further details can be found elsewhere [30,31]. The function ${}_1F_2(a;b_1,b_2;x)$ is introduced as the power series

$${}_1F_2(a;b_1,b_2;x) = \sum_{k=0}^{\infty}\frac{(a)_k}{(b_1)_k(b_2)_k}\frac{x^k}{k!}, \quad (A1)$$

where it is assumed that none of the parameters b_1 and b_2 is a nonpositive integer. Here $(a)_k$, $(b_1)_k$, and $(b_2)_k$ are Pochhammer symbols defined as $(\mu)_0 = 1$ and $(\mu)_k = \mu(\mu+1)\cdots(\mu+k-1) = (\mu+k-1)!/(\mu-1)!$. The power series of Eq. (A1) converges for all finite values of x and defines an entire function. The generalized hypergeometric function ${}_1F_2(a;b_1,b_2;x)$ satisfies the differential equation (9). In the neighborhood of the origin there are three linearly independent solutions to this equation. When neither of b_1, b_2 or $b_1 - b_2$ is an integer a fundamental set of solutions to Eq. (9) is given by

$$f_1(x) = {}_1F_2(a;b_1,b_2;x), \tag{A2a}$$

$$f_2(x) = x^{1-b_1}{}_1F_2(a-b_1+1;2-b_1,b_2-b_1+1;x), \tag{A2b}$$

$$f_3(x) = x^{1-b_2}{}_1F_2(a-b_2+1;b_1-b_2+1,2-b_2;x). \tag{A2c}$$

In this case, the general solution of Eq. (9) is given by

$$w(x) = Af_1(x) + Bf_2(x) + Cf_3(x). \tag{A3}$$

It can be shown [30,31] that the Wronskian of these solutions is given by

$$W[f_1(x),f_2(x),f_3(x)] = (b_1-1)(b_2-1)(b_1-b_2)x^{-b_1-b_2-1}. \tag{A4}$$

Some useful and important formulas could be derived from the definition (A1). For example,

$${}_1F_2(a;b_1,b_2;0) = 1. \tag{A5}$$

The derivative of GHF with respect to the independent variable x reads

$$\frac{d^n}{dx^n}{}_1F_2(a;b_1,b_2;x) = \frac{(a)_n}{(b_1)_n(b_2)_n}{}_1F_2(a+n;b_1+n,b_2+n;x). \tag{A6}$$

The derivatives of GHF with respect to the parameters are given by

$$\frac{d}{da}{}_1F_2(a;b_1,b_2,x) = -\psi(a){}_1F_2(a;b_1,b_2,x) + \sum_{k=0}^{\infty}\frac{(a)_k\psi(k+a)x^k}{(b_1)_k(b_2)_kk!}, \tag{A7a}$$

$$\frac{d}{db_j}{}_1F_2(a;b_1,b_2,x) = \psi(b_j){}_1F_2(a;b_1,b_2,x) - \sum_{k=0}^{\infty}\frac{(a)_k\psi(k+b_j)x^k}{(b_1)_k(b_2)_kk!} \quad (j=1,2). \tag{A7b}$$

The asymptotic expansion of GHF for $|x| \gg 1$ reads

$${}_1F_2(a;b_1,b_2;x) \sim \frac{\alpha^{-2a}\Gamma(b_1)\Gamma(b_2)}{\Gamma(b_1-a)\Gamma(b_2-a)}[1+O(\alpha^{-2})] + \frac{\alpha^{2\chi}\Gamma(b_1)\Gamma(b_2)}{2\sqrt{\pi}\Gamma(a)}\cos(\pi\chi+2\alpha)[1+O(\alpha^{-1})], \tag{A8}$$

where $x=-\alpha^2$ and $\chi = \frac{1}{2}(a-b_1-b_2+\frac{1}{2})$.

[1] B. W. Shore, *The Theory of Coherent Atomic Excitation* (Wiley, New York, 1990).
[2] B. W. Shore, J. Mod. Opt. **61**, 787 (2014).
[3] I. I. Rabi, Phys. Rev. **51**, 652 (1937).
[4] L. D. Landau, Phys. Z. Sowjetunion **2**, 46 (1932).
[5] C. Zener, Proc. R. Soc. A **137**, 696 (1932).
[6] E. C. G. Stückelberg, Helv. Phys. Acta **5**, 369 (1932).
[7] E. Majorana, Nuovo Cimento **9**, 43 (1932).
[8] N. Rosen and C. Zener, Phys. Rev. **40**, 502 (1932).
[9] Y. N. Demkov, Sov. Phys. JETP **18**, 138 (1964).
[10] N. V. Vitanov, J. Phys. B **26**, L53 (1993); **26**, 2085 (1993).
[11] E. E. Nikitin, Opt. Spectrosc. (USSR) **13**, 431 (1962); Adv. Quantum Chem. **5**, 135 (1970).
[12] N. V. Vitanov, J. Phys. B **27**, 1791 (1994).
[13] L. Allen and J. H. Eberly, *Optical Resonance and Two-Level Atoms* (Dover, New York, 1975).
[14] F. T. Hioe, Phys. Rev. A **30**, 2100 (1984).
[15] A. Bambini and P. R. Berman, Phys. Rev. A **23**, 2496 (1981).
[16] Y. N. Demkov and M. Kunike, Vestn. Leningr. Univ. **16**, 39 (1969).
[17] F. T. Hioe and C. E. Carroll, Phys. Rev. A **32**, 1541 (1985).
[18] J. Zakrzewski, Phys. Rev. A **32**, 3748 (1985).
[19] K.-A. Suominen and B. M. Garraway, Phys. Rev. A **45**, 374 (1992).
[20] C. E. Carroll and F. T. Hioe, J. Phys. A **19**, 3579 (1986).
[21] L. S. Simeonov and N. V. Vitanov, Phys. Rev. A **89**, 043411 (2014).
[22] E. Barnes and S. Das Sarma, Phys. Rev. Lett. **109**, 060401 (2012).
[23] N. V. Vitanov and B. W. Shore, J. Phys. B **48**, 174008 (2015).
[24] F. Bloch, Phys. Rev. **70**, 460 (1946).
[25] R. P. Feynman, F. L. J. Vernon, and R. W. Hellwarth, J. Appl. Phys. **28**, 49 (1957).
[26] E. S. Kyoseva and N. V. Vitanov, Phys. Rev. A **71**, 054102 (2005).
[27] Y. Avishai and Y. B. Band, Phys. Rev. A **90**, 032116 (2014).
[28] P. A. Ivanov and N. V. Vitanov, Phys. Rev. A **71**, 063407 (2005).
[29] X. Lacour, S. Guérin, L. P. Yatsenko, N. V. Vitanov, and H. R. Jauslin, Phys. Rev. A **75**, 033417 (2007).
[30] http://functions.wolfram.com
[31] E. D. Rainville, *Special Functions* (Macmillan, New York, 1960).
[32] P. A. Ivanov and D. Porras, Phys. Rev. A **88**, 023803 (2013).
[33] P. A. Ivanov, K. Singer, N. V. Vitanov, and D. Porras, arXiv:1506.07993 [quant-ph].
[34] K. Kim, M.-S. Chang, S. Korenblit, R. Islam, E. E. Edwards, J. K. Freericks, G.-D. Lin, L.-M. Duan, and C. Monroe, Nature (London) **465**, 590 (2010).
[35] A. Friedenauer, H. Schmitz, J. T. Glueckert, D. Porras, and T. Schaetz, Nat. Phys. **4**, 757 (2008).
[36] E. E. Edwards, S. Korenblit, K. Kim, R. Islam, M.-S. Chang, J. K. Freericks, G.-D. Lin, L.-M. Duan, and C. Monroe, Phys. Rev. B **82**, 060412(R) (2010).
[37] G. Heinze, C. Hubrich, and T. Halfmann, Phys. Rev. Lett. **111**, 033601 (2013).
[38] N. V. Vitanov and P. L. Knight, J. Phys. B **28**, 1905 (1995).
[39] B. Shore and N. Vitanov, Contemp. Phys. **47**, 341 (2006).